CHAPTER 163

OSClLLATORY FLOW BEHAVIOR IN THE
VlCINITY OF RlPPLE MODELS

Kiyoshi Horikawa[1] F. ASCE
Suguru Mizutani[2]

ABSTRACT

In the previous paper, a fixed ripple model with a
sharp crest was used to investigate the characteristics
of oscillatory flow in the vicinity of wavy boundary.
The above ripple model is useful to proof the
adaptability of the analytical treatment presented by
Longuet-Higgins (1981) and to extend our knowledge on the
present subject. However the stated model is too simple
to represent the real shape of sand ripples appeared on
the sea bottom. From such a view point, in the present
study another fixed ripple model with a round crest was
selected. This model has the shape almost similar to the
previous one except in the vicinity of the crest.

A two-dimensional LDV was used to measure the flow
velocity at preset grid points. By using these velocity
data the vorticity at each grid point was calculated and
the equivorticity lines were drawn for the sharp crest
ripple as well as the round crest ripple at various
phases of oscillatory flow. Then the circulation outside
the vortex was evaluated. Based on the available data
the temporal variation of the circulation was discussed
quantitatively. Finally criteria of vortex formation
were introduced and the physical meaning of these
criteria was discussed.

---

1. President, Saitama University, 255 Shimo-Okubo, Urawa,
   Saitama 338, Japan.
2. Postgraduate, Department of Foundation Engineering,
   Graduate School of Science and Engineering, Saitama
   University, 255 Shimo-Okubo, Urawa, Saitama 338, Japan.

INTRODUCTION

This paper is a continued work to the previous paper on the characteristics of oscillatory flow over a ripple model (Horikawa and Ikeda, 1990). In the foregoing paper were presented the extensive results of laboratory investigations carried out by using an oscillatory flume in which a fixed ripple model with a sharp crest was installed.
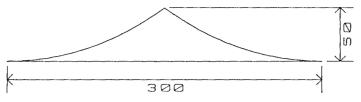
Figure 1 shows the shape and size of the stated model which were determined on the basis of the treatment presented by Longuet-Higgins (1981). This ripple model seems to be quite useful to analyze the flow phenomena in the vicinity of a wavy boundary. However the shape with such a sharp crest as this model may be unrealistic as a model of sand ripples appeared on the sea bottom. In order to investigate the actual flow phenomena in the vicinity of sand ripples generated by wave action, a more realistic model was selected.

According to Sleath (1984), the shape of two-dimensional vortex ripples for fine sand can be well expressed by the following equations :

$$y = (Hr/2) \cos kr\xi$$

$$\xi = x + (Hr/2) \sin kr\xi \tag{1}$$

where (x,y) are the Cartesian coordinates, ξ is the curvilinear coordinate following the wavy boundary with its origin at $x=0$ and $y=Hr/2$, Hr and Lr are the ripple height and the ripple length respectively, and $kr=2\pi/Lr$ is the ripple wave number as shown in Figure 2.

In order to keep the continuity and consistency in the series of research work, the ripple length was fixed at 30cm as that of the sharp crest ripple model. The ripple height of the new model was selected to be 4cm instead of 5cm in the previous model to make the height-length ratio 0.133 which is nearly equal to that of natural sand ripples. The shape of the new ripple model thus determined is shown in Figure 3. Figure 4 indicates the difference of both models. That is to say, the overall features of both models are practically similar each other except in the limited region of ripple crests.

(Unit:mm)

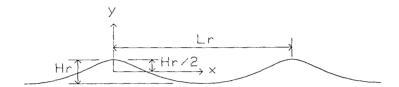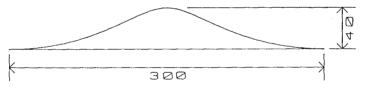Fig.1   Fixed ripple model with a sharp crest.

Fig.2   Definition sketch of sand ripple profile.

(Unit:mm)

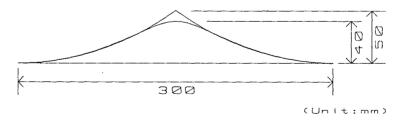Fig.3   Fixed ripple model with a round crest.

(Unit:mm)

Fig.4   Comparison of both fixed ripple models.

EXPERIMENTAL PROCEDURES

Experimental Conditions

    Table 1 gives the experimental conditions adopted   so
far at the Hydraulic Laboratory,   Saitama   University   by
using the fixed ripple model with a sharp   crest   (Figure
1) as   well   as   that   with   a   round   crest   (Figure   3)
installed inside an oscillatory flow flume   with   13m   in
length and 0.3m x 0.3m in   cross-section.   Among   these,
four particular cases namely Cases A, B, C and D in Table
1   will   be   selected   in   discussing   the   characteristic
differences of organized vortices formed behind   the   two
kind ripple crests.   Particularly in Cases A   and   B   the
oscillatory flow conditions are the same, but the   shapes
of the ripple crest are different each other.

Table 1   Experimental conditions.

Profile		T (s)	3	4	6		9
Sharp	d_0 (cm)	20.0	—	20.0	40.0	40.0
	U_{max} (cm/s)	20.9	—	10.5	20.9	13.9
		(Case C)				(Case A)
Round	d_0 (cm)	—	44.0	—		40.0
	U_{max} (cm/s)	—	34.6	—		13.9
			(Case D)			(Case B)

    d_0 :orbital total amplitude of fluid just outside the boundary layer at the bed
    U_{max}:amplitude of free stream horizontal velocity component

Experimental Apparatus and Flow Data Analysis

    A 2-D LDV was used to measure horizontal and vertical
components of flow velocity at each preset grid point   at
various   phases   of   oscillatory   flow.   By   using   the
obtained records various physical quantities such as   the
temporally   averaged   fluid   velocity,   stationary   (or
residual)   velocity,   kinematic   Reynolds   stress,   and
kinematic   eddy   viscosity,   were   calculated   and   the
resulted data were plotted in figures to   illustrate   the
temporal and spatial variations of flow   characteristics.
The detailed descriptions of   the   experimental   appratus
and   data   processing were given in   the   previous   paper
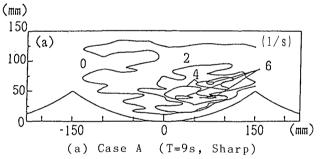(Horikawa and Ikeda, 1990).

    The   main   topic   in   this   paper,   however,   is   to
investigate the characteristic behavior of   an   organized
vortex formed behind a ripple crest.   The   discussion   on

fine structures of oscillatory flow in the vicinity of
ripple crest either with the sharp crest or with the
round crest will be made in the forthcoming paper which
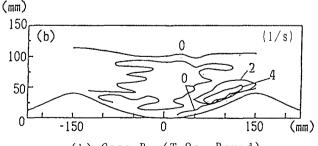is now in preparation.

BEHAVIOR OF AN ORGANIZED VORTEX

Overall Pattern of Vorticity

    Evaluation of vorticity at each grid point was made
by using the temporally averaged velocity components at
four grid points surrounding the prescribed point. As a
typical example, spatial distribution patterns of
vorticity for Cases A and B at the same phase of the
oscillatory flow are shown in Figures 5(a) and (b)
respectively. The irregularity of distribution patterns
is thought to be strongly influenced by the grid spacing
of measuring points.

    Comparing these two diagrams in Figure 5, it is
easily realized that the vorticity formed behind the

(a) Case A (T=9s, Sharp)

(b) Case B (T=9s, Round)

Fig.5   Spacial distribution of vorticity at the phase of
         $\omega t = 0$.
         [(a) Sharp crest ripple   (b) Round crest ripple]

sharp crest (Case A) is stronger than that behind the
round crest (Case B) as it is expected. In order to draw
more clear pictures, the following treatments were made.
The space area enclosed by the equivorticity curve with
the prescribed value was calculated at each phase. The
obtained values were plotted as indicated in Figures 6(a)
and (b) for Cases A and B respectively. From these
diagrams the following fact can be easily observed. Here
the phases $-\pi/2$ and $\pi/2$ correspond to the phases at the
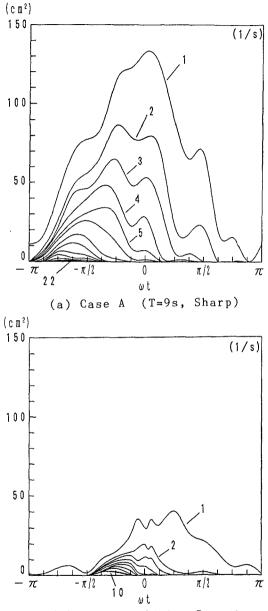maximum free stream velocity.

In case of the sharp crest ripple (Case A) the flow
streamline along the ripple bed separates definitely at
the crest. The vortex thus formed grows up with the
increase of free stream velocity and then diffuses rather
rapidly. Finally the overall vorticity decays due to
reverse of the free stream direction.

On the other hand, in case of the round crest ripple
(Case B) the size of vortex seems to be fairly small in
general compared with the previous one. The streamline
along the ripple bed separates hardly at the early stage
of oscillatory flow phase, but does at a certain phase
stage. The vortex area increases up to a certain phase
and then decreases gradually.

In both cases, the developing, diffusing and decaying
processes of vorticity can be observed clearly in Figures
6 (a) and (b). Even though the magnitude and spacial
scale of vortex depend strongly upon the shape of ripple
crest and free flow conditions, the processes stated
above appears similarly in any case.

In order to investigate the growth and decay of
overall vortex strength, the integrated vorticity with
respect to the area for Cases A, B, C and D were
calculated and the obtained values were plotted in Figure
7. The above integrated vorticity corresponds to the
circulation outside the vortex, Γ. From Figure 7 the
following can be pointed out :

(1) In case of the sharp crest ripple (Cases A and C),
    the flow separation initiates immediately after
    changing the flow direction. Then the circulation
    increases very rapidly and reaches its maximum, Γ max,
    at the phase of $-(\pi/4)$, a little after the
    maximum velocity of free stream. After that the

(a) Case A   (T=9s, Sharp)

(b) Case B   (T=9s, Round)
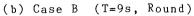
Fig.6   Temporal variation of the area   occupied   by   the
        vortex with the prescribed vorticity. [Case A   :
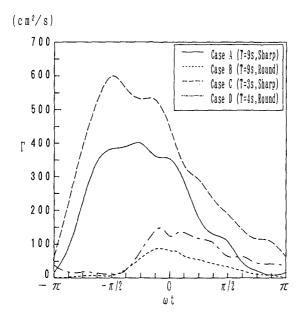   Sharp crest ripple   Case B : Round crest ripple]

Fig.7   Temporal variation of circulation outside the vortex generated behind a ripple crest.
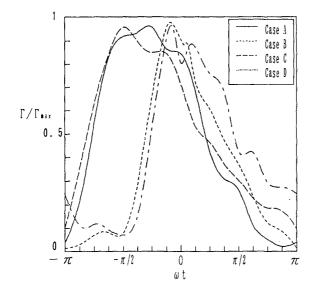

Fig.8   Temporal variation of nondimensional circulation.

circulation decreases gradually to zero at the phase
of π .
(2) In case of the round crest ripple (Cases B and D),
the flow separation appears at the phase of $-(\pi/2)$.
The circulation increases rather rapidly and reaches
its maximum at the phase of $-(\pi/8)$. Then the
circulation decreases gradually to zero.

In order to determine the general form of the
temporal variation of the circulation for both the
sharp crest ripple and the round ripple crest, the term
Γ/Γ max is illustrated in Figure 8, where Γ max is the
maximum value of Γ for each case. These curves suggest
us that the temporal variation of the circulation can
be expressed by an appropriate curve for each ripple
model. To accomplish the above treatment, the absolute
value of Γ max should be determined.

Available data of the maximum value of circulation
were summarized in Table 2. The first four data were
reported by Ikeda et al. (1988) who used the sharp crest
ripple with Hr/Lr=0.167. The second four data were given
by Sawamoto et al. (1980) who used the round crest ripple
with Hr/Lr=0.100 installed in an oscillatory air flume.
The last four data are those of Cases A, B, C and D in
the present investigation, where the values of Hr/Lr are
0.167 for Cases A and C and 0.133 for Cases B and D.

Table 2   Available   data   of   maximum   circulation.

T (s)	U_{max} (cm/s)	d_0 (cm)	L, (cm)	H, (cm)	Γ_{max} (cm²/s)	$\frac{H_r}{L_r}$	$\frac{TU_{max}}{H_r}$	$\frac{\Gamma_{max}}{TU_{max}^2}$	$\frac{U_{max}H_r}{\nu}$	
3	43.5	41.5	30	5	1500	0.167	26.1	0.264	2.18×10^4	I.S.
6	21.6	41.5	30	5	670	0.167	25.9	0.239	1.08×10^4	I.S.
9	14.5	41.5	30	5	555	0.167	26.1	0.293	7.25×10^3	I.S.
12	10.9	41.5	30	5	250	0.167	26.2	0.175	5.45×10^3	I.S.
6.4	49.0	200	50	5	2100	0.100	62.7	0.137	1.63×10^3	S.R.
6.4	29.5	120	50	5	656	0.100	37.8	0.118	9.89×10^2	S.R.
6.4	36.8	150	50	5	1172	0.100	47.1	0.135	9.89×10^2	S.R.
6.4	61.4	250	50	5	1640	0.100	78.6	0.068	2.05×10^3	S.R.
9	13.9	40.0	30	5	417	0.167	25.0	0.240	6.95×10^3	H.S.
3	20.9	20.0	30	5	626	0.167	12.5	0.478	1.05×10^4	H.S.
9	13.9	40.0	30	4	91	0.133	31.3	0.052	5.56×10^3	H.R.
4	34.6	40.0	30	4	154	0.133	34.6	0.032	1.38×10^4	H.R.

Ikeda et al.   Sharp   →   I.S.
Sawamoto et al.   Round   →   S.R.
Horikawa et al.   Sharp   →   H.S.
Horikawa et al.   Round   →   H.R.

Two nondimensional terms, $\Gamma max/(TUmax^2)$ and UmaxHr/ν, were correlated each other in Figure 9, where the effect of ripple model characteristics on the circulation was clearly distinguished. The scattering of data points is fairly large probably due to the fact that the applied evaluation methods for circulation are largely different each other. Therefore tentatively evaluated values are suggested by dotted lines in Figure 9. The ranges of the Reynolds number Re=UmaxHr/ν and the Keulegan-Carpenter number KC=TUmax/Hr are limited in each group of data (see Table 2). It is needless to say that additional data in a wide range of Re and KC are required to make more clear evaluation of the maximum circulation value under the various conditions.

Adaptability of the Present Data

In the previous investigations, the relationship among the grain size, the driving force of fluids, and the resulted sand ripple size was ignored. In order to keep the consistency of laboratory investigations the
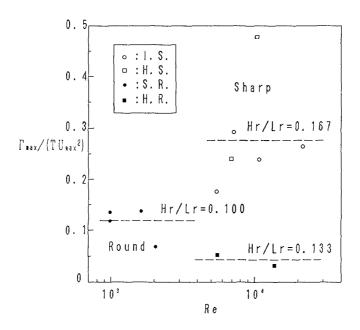

Fig.9   Tentative evaluation of maximum circulation.

oscillatory flow conditions were determined by using   two
types of empirical diagrams   presented   by   Mogridge   and
Kamphuis (1972)   and   Sato (1987) respectively   under the
conditions of Hr=4cm, Lr=30cm, and D=0.4mm.   Here   D   is
the   grain   size   of   sand.   The   flow   conditions   thus
obtained are   T=4s and   Umax=30cm/s   which correspond   to
the condition of Case D in the present experiments.

    Figure 10 gives the cumulative   grain   size   of   sand
particles   adopted   to   the   following   experiment.   The
medium grain size of D50=0.43mm is nearly   equal   to   the
expected value of 0.4mm.   Figure 11 shows the   comparison
between the profile of fixed ripple model with the   round
crest   and   the   measured   profile   of   the   sand   ripple
generated in the oscillatory flow flume.   The   agreement
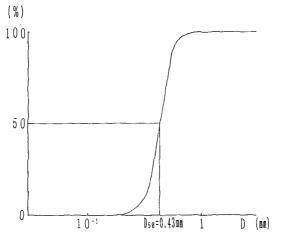seems to be extremely good.

Fig.10   Cumulative grain size   curve   of   sand   particles
         used for the laboratory experiment.
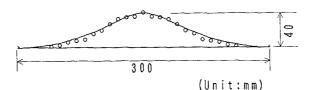
Fig.11   Comparison of measured sand ripple profile   with
         the fixed ripple model.

Criteria of Organized Vortex Formation

     Again the fixed model of ripple with the round crest
was installed in the oscillatory flume and the maximum
horizontal size of organized vortices was measured
visually by using a scale under the numerous combinations
of period and amplitude of the piston stroke.   The
measured data were plotted on a diagram with the abscissa
of Reynolds number, Re, and the ordinate of Keulegan-
Carpenter number, KC, as shown in Figure 12.   Different
symbols were used to indicate roughly the vortex size.

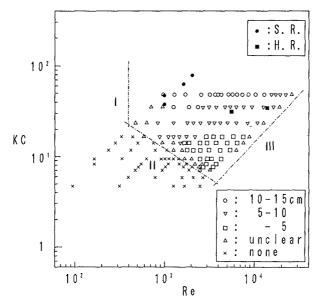
Fig.12 Criterion Curves I, 11 and IlI for vortex
        formation (fixed ripple model with the round
        crest).

     In this figure three different curves denoted by 1,
11 and 111 were drawn as criteria of vortex formation.
The physical meaning of these three curves will be
discussed in the following :

(1) Curve 1 shows that the Reynolds number should exceed
    a certain number to generate the organized vortex.
    The possible minimum value of the Reynolds number
    might be 400.
(2) Curve 1I corresponds to the following condition. 1t
    is well known that the Strouhal number of the vortex

shedding induced to a circular cylinder in a steady
flow depends upon the Reynolds number. The KC number
in the present investigation corresponds to the
receiprocal of Strouhal number. Therefore it seems
to be natural that the critical KC number for vortex
formation depends upon the Reynolds number.

(3) Sleath (1984) introduced the following relationship
for any given sediment to determine the wavelength Lr
of the rolling grain ripples

$$\beta Lr = \alpha = \text{constant} \qquad (2)$$

where $\beta = \sqrt{\omega/2\nu}$, $\omega = 2\pi/T$, and ν is the kinematic
viscosity of fluid. Transformation of Equation (2)
yields

$$KC = \frac{\pi}{\alpha^2 (Hr/Lr)^2} \; Re \qquad (3)$$

In the present case Hr/Lr=0.133, hence the KC number
is proportional to the Reynolds number. Based on the
above discussion, Curve III may be closely related
to the criterion of rolling grain ripple formation.

The experimental conditions of the Sawamoto et al.
cases, and Cases B and D in the present investigations
fall within the region of vortex formation as
demonstrated in Figure 12.

CONCLUSIONS

In this paper the characteristics of the organized
vortex formed behind a ripple crest in an oscillatory
flow were investigated in detail. Two ripple models were
adopted for the present study ; the first is the ripple
model with a sharp crest and the second is that with a
round crest. The main conclusions are as follows :

1) The vorticity of the organized vortex induced by the
   sharp crest ripple is naturally stronger than that by
   the round crest ripple.
2) The circulation outside the vortex region was
   evaluated for each phase of oscillatory flow. The
   nondimensionalized circulation has temporally a
   specified form for each type of ripple profile. In

order to determine clearly the variational form with
the phase of oscillatory flow, additional data are
needed.
3) Vortex formation due to the round crest ripple was
clearly observed in a certain region in the domain of
the Reynolds number versus the Keulegan-Carpenter
number. The physical meaning of the three criteria
was described.

REFERENCES

Horikawa, K. and S. Ikeda : Characteristics of oscil-
latory flow over ripple models, Proc. 22nd Coastal
Engineering Conference, ASCE, pp.661-674, 1990.

Ikeda, S., S. Kisaki, and S. Kurihara : Modelling of
oscillatory flow and vortices in the vicinity of sand
ripple, Proc. 35th Japanese Conference on Coastal
Engineering, pp.21-24, 1988 (in Japanese).

Longuet-Higgins, M. S. : Oscillatory flow over steep sand
ripples, Journal of Fluid Mechanics, Vol.107, pp.1-
35, 1981.

Mogridge, G. R. and J. W. Kamphuis : Experiments on bed
form generation by wave action, Proc. 13th Conf. on
Coastal Engineering, ASCE, pp.1123-1142, 1972.

Sleath, J. F. A. : Sea Bed Mechanics, John Wiley & Sons,
p.128, 1984.

Sato, S. : Oscillatory boundary layer flow and sand
movement over ripples, Dr. Eng. Dissertation, Univer-
sity of Tokyo, Japan, 1987.

Sawamoto, M., T. Yamashita and T. Kurita : Vortex
formation over rippled bed under oscillatory flow,
Department of Civil Engineering, Tokyo Institute of
Technology, Technical Report No.27, pp.75-85, 1980.